https://doi.org/10.3311/PPee.37002

Periodica Polytechnica Electrical Engineering and Computer Science, 68(4), pp. 327–334, 2024

Iterative Numerical Approximation Technique for 3D Eddy Current Models in Harmonic Regime Based on the Electromagnetic *T*-Formulation and the Finite Element Method

Nabil Benhadda[1,4*], Dahmane Hachi[2], Bachir Helifa[3], Bachir Abdelhadi[4], Ibn Khaldoun Lefkaier[3]

[1] Department of Industrial Engineering, Faculty of Science and Technology, University of Abbes Laghrour, Khenchela, PB 1252 Road of Batna, Khenchela, 40004 Khenchela, Algeria
[2] Laboratory of Development in Mechanics and Materials (LDMM), University of Djelfa, P.O.B 3117, Road of Moudjbara Djelfa, 17000 Djelfa, Algeria
[3] Materials Physics Laboratory, University of Laghouat, BP 37G, Road of Ghardaia 37G Laghouat, 03000 Laghouat, Algeria
[4] Laboratory of Electric Traction Systems (LSTE – Batna 2), Electrical Engineering Department, Faculty of Technology, University Batna 2, Road of Constantine 53, Fésdis, P.O.B 05078, Batna, Algérie
* Corresponding author, e-mail: benhadda_nabil@univ-khenchela.dz

Received: 30 March 2024, Accepted: 20 September 2024, Published online: 30 September 2024

Abstract

In this paper, an iterative numerical approximation technique is used for analyzing the distribution of eddy currents density in conductive materials plates by using the electromagnetic *T*-formulation and the Biot-Savart law, solved by the finite element method. The proposed approach allows for the meshing of the different parts of the studied system separately, including the sensor and the conductive plate, without the need for an air region. Firstly, this approach reduces the number of unknown variables by avoiding the air region of the system's mesh. Secondly, it simplifies the consideration of the sensor's motion without the need to remesh the system. For this purpose, a calculation code has been developed for solving an electromagnetic three-dimensional non-destructive testing model. This latter permits the resolution of JSEAM # 6 Benchmark problem to validate the proposed method. The impedance variation due to the presence of a defect are evaluated. The obtained results are compared with the experimental ones found in the literature. These results reveal a good agreement, which proves the validity of the proposed method.

Keywords

eddy currents, 3D finite elements method, *T*-formulation, *T*-iterative, non-destructive testing (NDT)

1 Introduction

The eddy current nondestructive testing (EC-NDT) is used to detect and quantify various surface defects in conductive materials [1, 2], i.e. to demonstrate the presence of heterogeneity in the controlled material. In the field of modeling, analytical approaches require a great electromagnetism knowledge, a considerable development time and a particular treatment for each geometric configuration [3–5].

The rapid evolution of computing and numerical computing techniques has helped to solve this problem. In fact, the finite element method is one of them since it allows the resolution of complex geometries [6–8].

In addition, it is actually heavy computing time, but quoted precision is the best compared to other methods. Therefore, to solve this dilemma, an iterative method that is based on the $\vec{T}$ formulation and the Biot-savart law will be associated with the finite element method to solve a problem of non-destructive evaluation (NDT) by eddy currents. The latter allows to separately partition the components of the studied system, consisting for the sensor and the conductive plate. This latter approach allows reducing the number of unknown variables by avoiding the air region of the overall system and allows for easily taking into account the motion of the sensor without remeshing the system.

Several scientific works, in the literature, use the $\vec{T}$-iterative method for modeling and simulating of problems of Eddy Current nondestructive Testing (EC-NDT) [9–12]. In 2009, [11] exploited this iterative method associated

Cite this article as: Benhadda, N., Hachi, D., Helifa, B., Abdelhadi, B., Lefkaier, I. K. "Iterative Numerical Approximation Technique for 3D Eddy Current Models in Harmonic Regime Based on the Electromagnetic *T*-Formulation and the Finite Element Method", Periodica Polytechnica Electrical Engineering and Computer Science, 68(4), pp. 327–334, 2024. https://doi.org/10.3311/PPee.37002

with the finite difference method to characterize composite carbon fiber materials (CFRP), and in 2012, [12] used the same method coupled with the finite volume method to characterize isotropic materials and CFRP composites possibly containing defects.

In this context, we have developed a Matlab calculation code based on the proposed method, to solve an EC-NDT problem that contains an absolute Pancake coil sensor above of a conductive plate with and without a defect. To mesh the geometry of the sensor/plate separately, the Gmsh software is used [13]. Moreover, the displacement of the coil is taken into consideration without remeshing the system. To test the proposed method, the obtained simulation results are compared with the experimental ones of the benchmark problem [14]. The work presented in this paper is divided into four sections and structured as follows: In the second section, we will illustrate the eddy current NDT device to be studied and the different governing equations. The third section will discuss the proposed method and its concept, as well as the flowchart, which contains the different steps of solving the magnetodynamic equation, the calculation of the eddy current density in a conductive plate, and the sensor impedance variation. In the last section of this article, two applications will be treated. The first application will study the eddy current distributions in an isotropic defect-free plate. The second application concerns the distributions of eddy currents in the same isotropic plate but with a defect. To validate this work and the effectiveness of the proposed method, we will compare the results obtained with the experimental results expressed in the JSEAM #6 benchmark.

2 Modelization of studied device

The problem of eddy currents NDT to be studied consists of an inductor (source) where the excitation ($\vec{J}_s$) is imposed and a conductive region representing the plate to be controlled in absence of air region, which makes it possible to minimize the mesh. The system is shown in Fig. 1.

2.1 Eddy current testing through Maxwell equations

Maxwell's equations describe the physical model used for electromagnetic EC problems solved with the finite element method (FEM) that allows determining the response of sensor eddy current. The magnetic vector potential, electric and magnetic field or the pointing vectors are the most quantities widely used to solve the field equations. Quasi-stationary Maxwell equations are given hereafter:

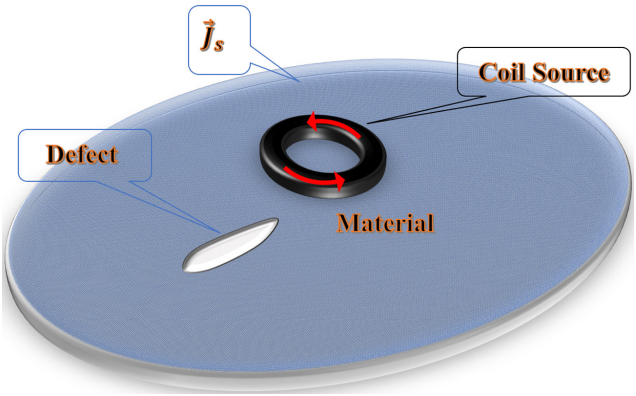

Fig. 1 Eddy current NDT system

$$\vec{\nabla}\times\vec{H}=\vec{J}+\frac{\partial\vec{D}}{\partial t}, \tag{1}$$

$$\vec{\nabla}\times\vec{E}=-\frac{\partial\vec{B}}{\partial t}, \tag{2}$$

$$\vec{\nabla}.\vec{D}=\rho, \tag{3}$$

$$\vec{\nabla}.\vec{B}=0. \tag{4}$$

The electric vector potential formulation $\vec{T}$ is based on the conservation law of the electric current which is given by:

$$\vec{\nabla}.\vec{J}=0 \text{ And } \vec{J}_i=\vec{\nabla}\times\vec{T}. \tag{5}$$

By replacing the Eq. (5) into Eq. (2), we obtain the following relation:

$$\vec{\nabla}\times\left(\vec{\vec{\sigma}}^{-1}\vec{\nabla}\times\vec{T}(r)\right)=-j\omega\left(\vec{H}\right), \tag{6}$$

with $\vec{H}$ is the intensity of the magnetic field that is given by the following expression:

$$\vec{H}=\vec{H}_s+\vec{H}_r, \tag{7}$$

where $\vec{H}_s$ and $\vec{H}_r$ are respectively the intensities of the magnetic field in a source and in the piece. The developed formulation is based on the $\vec{T}$ formula given by Eq. (6), and the Biot-Savart law which is expressed by the following Eq. (10) and Eq. (11):

$$\vec{H}_s(r)=\frac{1}{4\pi}\int_{\Omega_s}\frac{\vec{J}_s(r_s)\times|\vec{r}-\vec{r}_s|}{|\vec{r}-\vec{r}_s|^3}d\Omega_s, \tag{8}$$

where r is the distance between a point situated in the source region and a point in the region that represents the plate, Ω_c is the volume in a source region. $\vec{H}_r$: Can be calculated by Biot-Savart law as follows:

$$\vec{H}_r(r) = \frac{1}{4\pi}\int_{\Omega_c} \frac{\vec{J}_i(r_c)\times|\vec{r}-\vec{r}_c|}{|\vec{r}-\vec{r}_c|^3} d\Omega_c \,. \tag{9}$$

$\vec{r}$ Represent the distance between two elements in the conductor and Ω_c is the volume of each element in conductor.

To solve this Eq. (6), we have used the $\vec{T}$ iterative method which was already proposed by some authors to calculate eddy currents in NDT problems [9, 12]. The advantage of this method uses a reduced number of unknown variables and the air is not including in the mesh of the global system. The flowchart of this method is illustrated in the Fig. 2.

In the first step, the induced current density is initialized to zero $\vec{J}_i = \vec{0}$ in each meshing element of the piece. Then, in the second step, we proceed to solving Eq. (6) in an iterative process using the equation $\vec{J}_i = \vec{\nabla}\times\vec{T}$ to calculate the new density of induced currents. In the third step, a convergence test has been carried out on all the real and imaginary parts separately in order to avoid that the imaginary part is included in the calculation error.

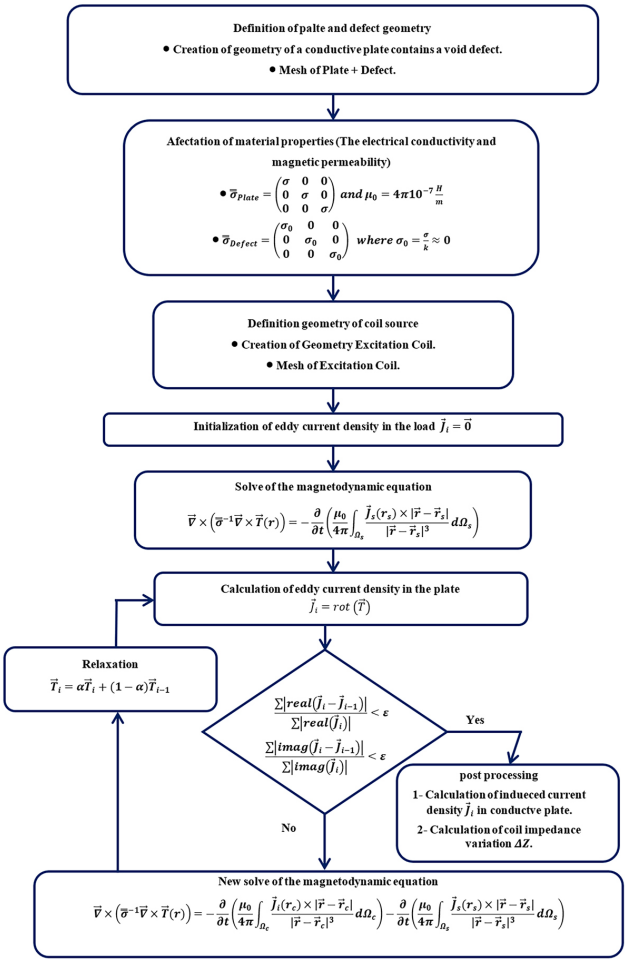

Fig. 2 Flowchart of the proposed iterative method

To control the convergence, a relaxation is used which expressed by:

$$\vec{T}_i = \alpha\vec{T}_i + (1-\alpha)\vec{T}_{i\text{-}1}. \tag{10}$$

Hence, the introduction of a factor α called "relaxation factor" such as « $0 \le \alpha < 1$ », [12, 15] aims to make it possible to ensure system convergence. The maximum convergence speed should be achieved with $\alpha = 1$. The algorithm may usually diverge, so a damped algorithm choosing a parameter « $0 \le \alpha < 1$ » improves stability (convergence) but at the cost of higher number of iterations, leading to a longer computation time. The process stops when the convergence is reached, the progress of the $\vec{T}$-iterative method is synthesized by the flowchart below:

2.2 Impedance calculation

There are several formulations in the literature for calculating impedance variation where the inductor is fed by a current I_s, the variation of its impedance due to the currents induced in the piece for a conductive material can be evaluated by the following expression [8, 16–17]:

$$\Delta R + j\Delta X = -\frac{1}{I_s^2}\int_{\Omega_s}\vec{E}_i\times\vec{J}_s d\Omega_s = -\frac{1}{I_s^2}\int_{\Omega_c}\vec{E}_s\times\vec{J}_i d\Omega_c, \tag{11}$$

where $\vec{E}_i$ represents the inverse electric field produced by the induced currents in the piece and $\vec{J}_s$ represents the source current density in the coil. Similarly, $\vec{E}_s$ represents the electric field in the source and $\vec{J}_s$ expresses the density of induced currents in the piece.

By using the Biot-Savart formula, we can evaluate the electric field $\vec{E}_i$. Finally, we obtain the following relation [11]:

$$\Delta Z = -\frac{j\omega\mu_0}{4\pi I_s^2}\int_{\Omega_s}\int_{\Omega_c}\frac{\vec{J}_i(\vec{r}_c)\times\vec{J}_s(\vec{r})}{|\vec{r}-\vec{r}_c|} d\Omega_c d\Omega_s \text{ and } \begin{pmatrix}\vec{r}\in\Omega_s\\ \vec{r}_c\in\Omega_c\end{pmatrix}, \tag{12}$$

where $|\vec{r}-\vec{r}'|$ is the distance between a point marked by the vector $\vec{r}'$ belonging to the region Ω_c and a point marked by the vector $\vec{r}$ belonging to the region Ω_c.

3 Applications

The eddy current non-destructive testing system (EC-NDT) can be modeled by the scheme shown in Fig. 3. A material representing the critical part and containing the defect is subjected to the action of an electromagnetic field produced by a coil forming the EC sensor, where a variable

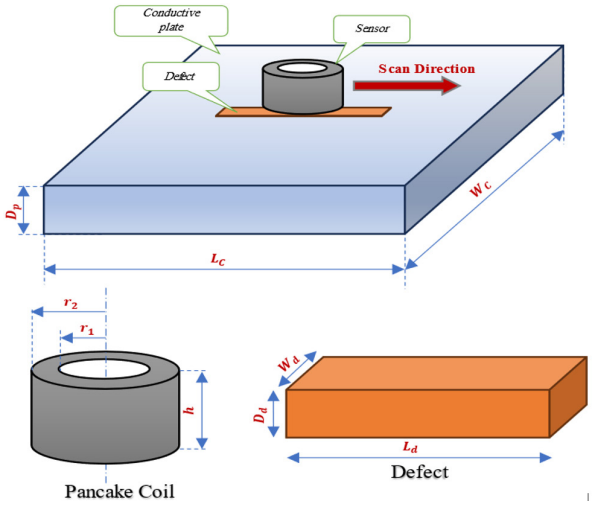

Fig. 3 Geometrical configuration of the studied device

current density is imposed. The objective is to evaluate the eddy currents in the plate when the coil impedance changes [18]. The simulation of the EC-NDT device is performed in the quasi-stationary harmonic regime.

The simulation of any electromagnetic system requires knowledge of all physical and geometrical characteristics in different regions. The physical and geometrical parameters of the system to be studied are given in Table 1.

The use of the ($\vec{T}$-iterative) formulation allows us to mesh the plate and the coil separately only once with a hexahydric mesh element. The coil is divided into 1792 volumes and the plate is divided into 8970 volumes. Air is not included. Fig. 4 and Fig. 5 represents the mesh of the plate and the coil respectively.

4 Results and validation

4.1 Isotropic plate without defect

First of all, we validated the developed code by using the ($\vec{T}$-iterative) formulation. The latter has the advantage that we only link the active zone compared to the other formulations (*AV* formulation and the *TΩ* formulation) [10].

Table 1 Physical and geometrical characteristics of the studied device [14]

Conductive Plate		Coil		Defect	
Length L_c	140	Inner radius r_1 (mm)	0.6	Length L_d (mm)	10
Width W_c	140	Outer radius r_2 (mm)	1.6	Depth D_d (mm)	0.75
Depth D_p	1.25	Length h (mm)	0.8	Width W_d (mm)	0.22
Electrical Conductivity σ(S/m)	10^6	Number of turns N	140	Frequency F_r (kHz)	150, 300
Magnetic Permeability μ_r	1	Lift-off L_f (mm)	0.5/1	I_s (mA)	0.7

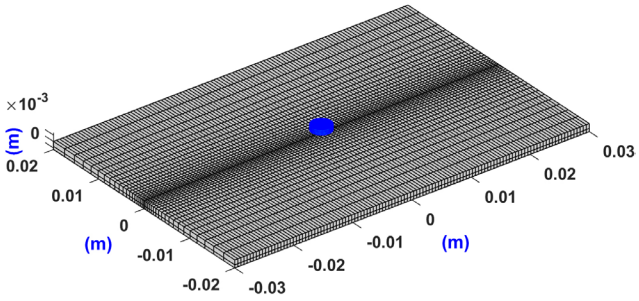

Fig. 4 3D mesh of the studied device

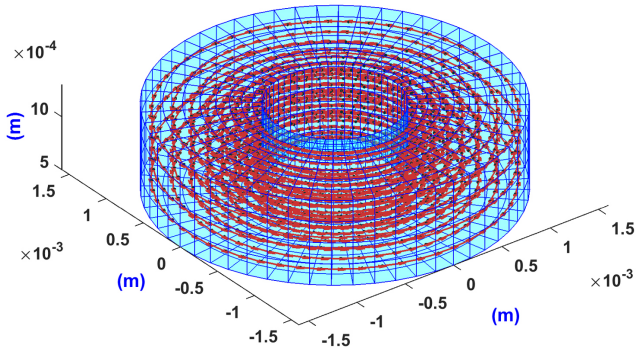

Fig. 5 Meshing of the coil and the distribution of the source current density

The disadvantage of this method appeared when we use Biot-Savart's law to calculate the magnetic field in the conductor created by the eddy currents, a memory problem appears straight away in MATLAB® because of the manipulation of high order matrix. To overcome this problem, we can transform this full matrix into a sparse matrix. We assume that eddy currents far from the coil create very little magnetic field and can therefore be neglected.

The variation of the impedance and the difference between the measured results and those simulated for two frequencies 150 kHz and 300 kHz with a lift-off of 0.5 mm are illustrated in Fig. 6 and Fig. 7.

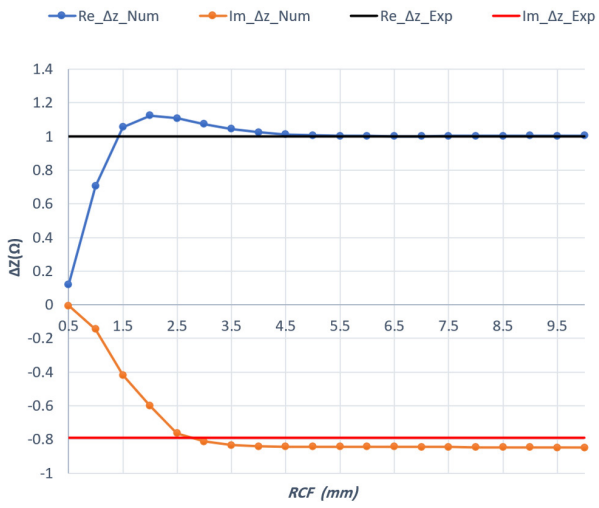

Fig. 6 Coil impedance variation as a function of the fictitious radius of the eddy currents (R_{CF}) for F_r = 150 kHz and L_f = 0.5 mm

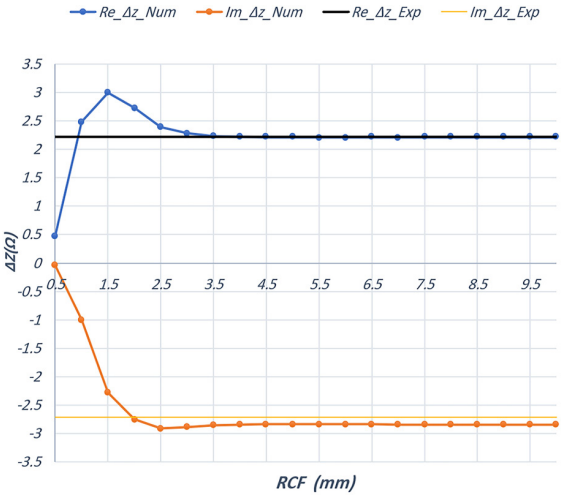

Fig. 7 Coil impedance variation as a function of the fictitious radius of the eddy currents (R_{CF}) for F_r = 300 kHz and L_f = 0.5 mm

From these figures, it can be seen that the impedance variations approach the measurement and begin to give the same result when the fictitious radius of the induced currents is greater than or equal to four or five R_o the external radius of the coil, such that:

$$R_{CF} = (4 \text{ to } 5) \times R_o, \tag{13}$$

where:

- R_{CF}: Fictitious radius of eddy currents
- R_o: External radius of the coil.

We can therefore limit the domain of study to more of (5 × Radius of coil) to get acceptable results.

The Fig. 8 presents the distribution of the densities of the induced currents as a function of the fictitious radius of the eddy currents. The same observation is observed, i.e., the

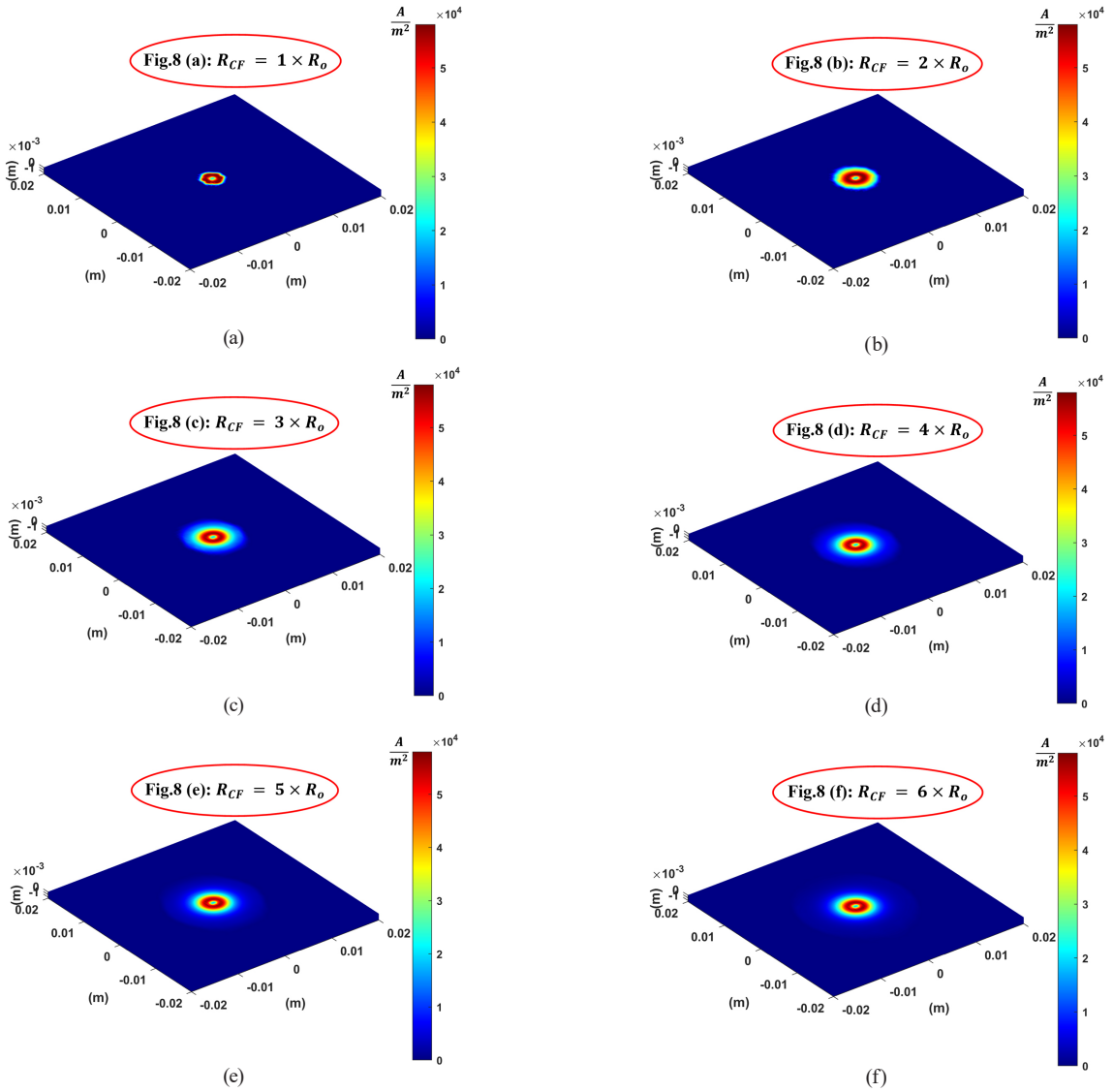

Fig. 8 Distribution of the density of the induced currents as a function of the fictitious radius, (a) The induced currents for $R_{CF} = 1 \times R_o$, (b) The induced currents for $R_{CF} = 2 \times R_o$, (c) The induced currents for $R_{CF} = 3 \times R_o$, (d) The induced currents for $R_{CF} = 4 \times R_o$, (e) The induced currents for $R_{CF} = 5 \times R_o$, (f) The induced currents for $R_{CF} = 6 \times R_o$

variation in the fictitious radius of the plate begins to give the same distribution of the densities of the induced currents when the fictitious radius of the induced currents is greater than or equal to four or five times, the external radius of the coil, as shown in Fig. 8 (a), (b), (c), (d), (e) and (f).

The table below shows the comparison between the experimental results presented in [14] and the results obtained by the code that we have developed using the finite element method associated with the $\vec{T}$-iterative technique.

The impedance calculated in a single point by the proposed method is compared with the one obtained experimentally for two frequencies 150 kHz and 300 kHz and for a lift-off of 0.5 and 1.0 mm [19]. The obtained results from ΔR and ΔX are grouped on Table 2. According to this table. We remark also that there are differences in the gap between the experimental results and those of the simulation. The error is more important in the imaginary part than the real one and this is due to the geometry discretization (mesh). But generally, one can see that there is a great accord between the experimental results and those of numerical ones.

4.2 Isotropic plate with defect

In the defect region, where the electrical conductivity tends to zero ($\sigma_{defect} = 0$), the inverse electrical conductivity tensor tends to infinity ($(\overline{\overline{\sigma_{ij}}}^{-1} = \infty$), causing a singularity in the studied system (Eq. (6)). In order to avoid the singularity of the system (divergence), holes and defects filled with non-conductive materials ($\sigma_{defect} = 0$) can be replaced by materials with very low conductivity ($\sigma_{defect} \approx 0$) relative to the conductivity of the conductive material. For example:

$$\sigma_{defect} = \frac{\sigma_{material}}{k}, \tag{14}$$

where k is constant), [20, 21], in order to avoid the singularity of the system (divergence). The simulation results for a plate with defect are obtained by the application of $\vec{T}$-iterative method as shows by the figures bellow where the displacement of the coil is taken into account.

The variation of real and the imaginer parts in the function of the movements of the coil is represented in the Fig. 9, Fig. 10, Fig. 11 and Fig. 12 respectively.

Table 2 Plate impedance variations [14]

L_f (mm)	F_r (KH)	ΔZ_{Exper} (Ω)	ΔZ_{Calcul} (Ω)
0.50	150	1.00 – j0.79	1.002 – j0.843
0.50	300	2.22 – j2.71	2.208 – j2.834
1.00	150	0.41 – j0.48	0.466 – j0.497
1.00	300	0.94 – j1.47	0.961 – j1.528

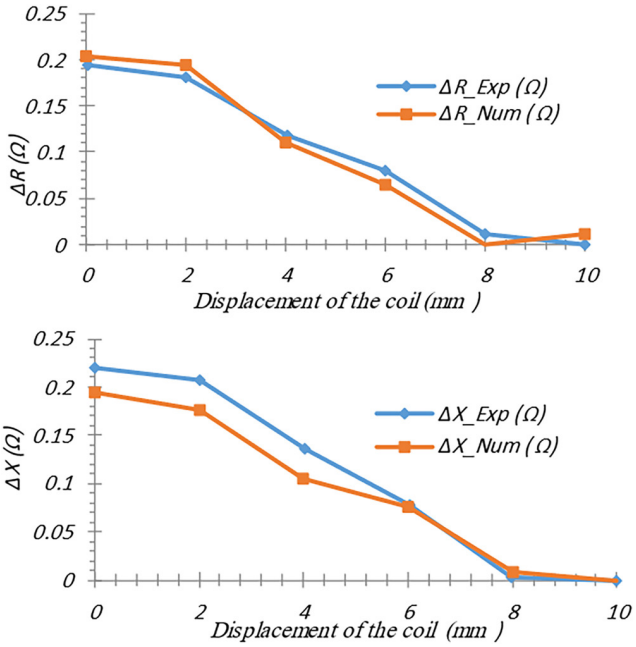

Fig. 9 Comparison between the experimental and the numerical results of the real and imaginary part of the impedance for F_r = 150 kHz and L_f = 0.5 mm

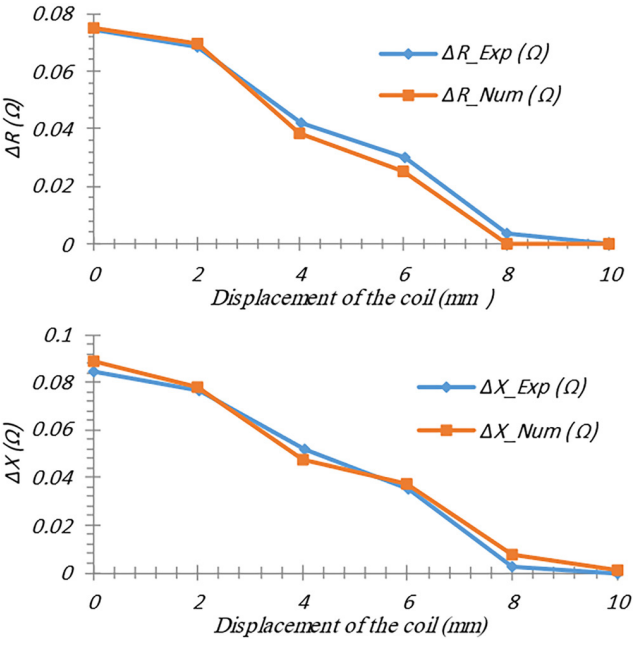

Fig. 10 Comparison between the experimental and the numerical results of the real and imaginary part of the impedance for F_r = 150 kHz and L_f = 1.0 mm

These figures show a comparison between the calculated values obtained with the proposed method and the measured results.

We can see that the impedance change becomes smaller when the coil is far from the center of the defect. When the letter is in a center of the defect the impedance variation is maximal. In author hand the variation of impedance is

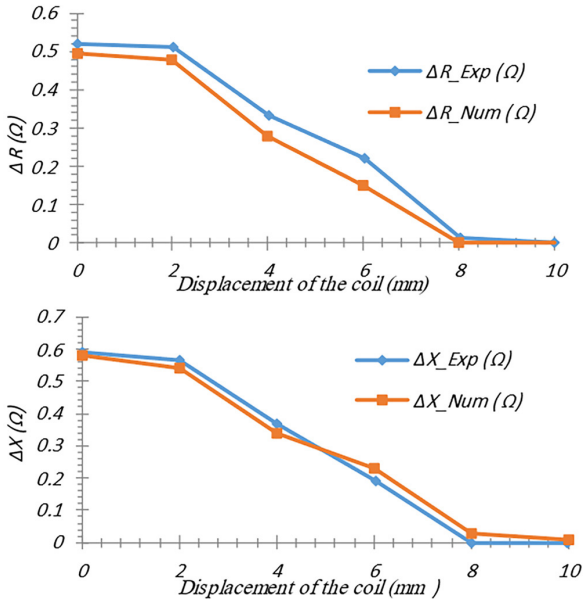

Fig. 11 Comparison between the experimental and the numerical results of the real and imaginary part of the impedance for F_r = 300 kHz and L_f = 0.5 mm

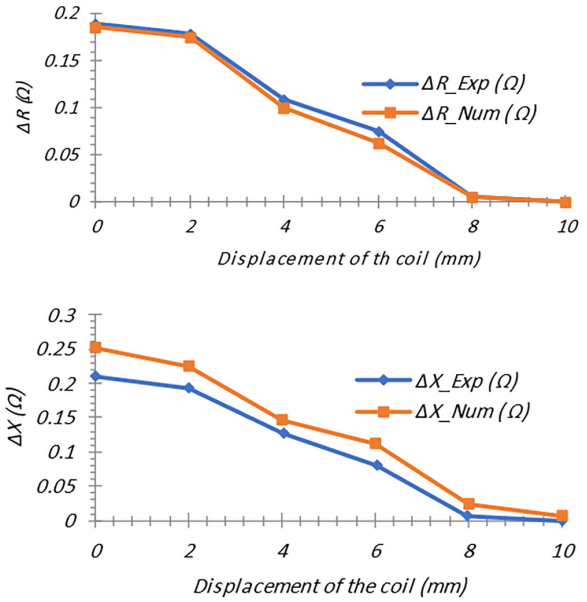

Fig. 12 Comparison between the experimental and the numerical results of the real and imaginary part of the impedance for F_r = 300 kHz and L_f = 1.0 mm

proportional to the frequency variation when the lift off is constant. In opposite, when the lift-off increases the variation of impedance decreased.

From the Fig. 13 we notice a discontinuity of eddy currents in the plate. It is due to the existence of a defect of rectangular shape. It is found that those currents circulate around the latter and that justify the effectiveness of the proposed method.

The calculation is performed on a PC with an Intel® Core (TM) I5–2450 M 2.5 GHz CPU and 8 GB of RAM. The algorithm uses 211 iterations when α = 0.1. The relative error is 10^{-6}. At each position of the coil the PC takes about 2.13 minutes to solve this problem.

5 Conclusion

Through this article, a nondestructive evaluation of a benchmark problem has been solved. We have developed a calculation code based on the $\vec{T}$-iterative method associated with the finite element method. The Biot-Savart law is a means we have used to avoid meshing the air when moving the sensor. Eddy currents were evaluated in the conductive plate with and without defect. The obtained simulation results were compared with the experimental ones. A great agreement was noticed between these results and justifies the utility of this method. In conclusion, the main contribution of this work lies in the utilization of the presented technique alongside experimental results, which enable testing the effectiveness and credibility of this technique.

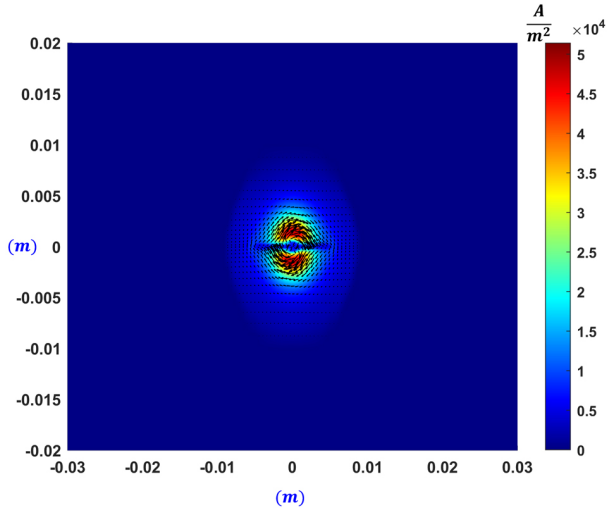

Fig. 13 Distributions of induced currents in the plate in the presence of a defect

References

[1] Benhadda, N., Hachi, D., Helifa, B., Lefkaier, I. K., Abdelhadi, B. "Development of multi-coils circular eddy current sensor for characterization of fibers orientation and defect detection in multidirectional CFRP material", Research in Nondestructive Evaluation, 31(3), pp. 133–146, 2020. https://doi.org/10.1080/09349847.2019.1645254

[2] Huang, H., Sakurai, N., Takagi, T., Uchimoto, T. "Design of an eddy-current array probe for crack sizing in steam generator tubes", NDT and E International, 36(7), pp. 515–522, 2003. https://doi.org/10.1016/S0963-8695(03)00050-1

[3] Burke, S. K. "Eddy-current induction in a uniaxially anisotropic plate", Journal of Applied Physics, 68(7), pp. 3080–3090, 1990. https://doi.org/10.1063/1.347171

[4] Li, Y., Chen, Z., Qi, Y. "Generalized analytical expressions of liftoff intersection in PEC and a liftoff-intersection-based fast inverse model", IEEE Transactions on Magnetics, 47(10), pp. 2931–2934, 2011. https://doi.org/10.1109/TMAG.2011.2148099

[5] Dodd, C. V., Deeds, W. E. "Analytical solutions to eddy-current probe-coil problems", Journal of Applied Physics, 39(6), pp. 2829–2838, 1968. https://doi.org/10.1063/1.1656680

[6] Rosell, A., Persson, G. "Finite element modelling of closed cracks in eddy current testing", International Journal of Fatigue, 41, pp. 30–38, 2012. https://doi.org/10.1016/j.ijfatigue.2011.12.003

[7] Santandréa, L., Le Bihan, Y. "Using COMSOL-multiphysics in an eddy current non-destructive testing context", in Proceedings of the COMSOL Conference 2010, Paris, France, Nov, 2010.

[8] Ida, N., Lord, W. "A finite element model for three-dimensional Eddy current NDT phenomena", IEEE Transactions on Magnetics, 21(6), pp. 2635–2643, 1985. https://doi.org/10.1109/TMAG.1985.1064207

[9] Takagi, T., Sugiura, T., Miyata, K., Norimatsu, S., Okamura, K., Miya, K. "Iterative solution technique for 3-D eddy current analysis using T-method", IEEE Transactions on Magnetics, 24(6), pp. 2682–2684, 1988. https://doi.org/10.1109/20.92212

[10] Takagi, T., Hashimoto, M., Arita, S., Norimatsu, S., Sugiura, T., Miya, K. "Experimental verification of 3D eddy current analysis code using T-method", IEEE Transactions on Magnetics, 26(2), pp. 474–477, 1990. https://doi.org/10.1109/20.106356

[11] Menana, H., Féliachi, M. "3-D eddy current computation in carbon-fiber reinforced composites", IEEE Transactions on Magnetics, 45(3), pp. 1008–1011, 2009. https://doi.org/10.1109/TMAG.2009.2012542

[12] Li, Y., Berthiau, G., Feliachi, M., Cheriet, A. "3D finite volume modeling of ENDE using electromagnetic T-formulation", Journal of Sensors, 2012(1), 785271, 2012. https://doi.org/10.1155/2012/785271

[13] Geuzaine, C., Remacle, J.-F. "Gmsh: A 3-D finite element mesh generator with built-in pre-and post-processing facilities", International Journal for Numerical Methods in Engineering, 79(11), pp. 1309–1331, 2009. https://doi.org/10.1002/nme.2579

[14] Shimone, J. "Impedance measurement of unique shape cracks by pancake type coil", Applied Electromagnetics, (5), pp. 12–17, 1996.

[15] Hachi, D., Benhadda, N., Helifa, B., Lefkaier, I. K., Abdelhadi, B. "Composite material characterization using eddy current by 3D FEM associated with iterative technique", Advanced Electromagnetics, 8(1), pp. 8–15, 2019. https://doi.org/10.7716/aem.v8i1.953

[16] Bowler, J. R., Sabbagh, L. D., Sabbagh, H. A. "A theoretical and computational model of eddy-current probes incorporating volume integral and conjugate gradient methods", IEEE Transactions on Magnetics, 25(3), pp. 2650–2664, 1989. https://doi.org/10.1109/20.24505

[17] Zaoui, A., Menana, H., Feliachi, M., Abdellah, M. "Generalization of the ideal crack model for an arrayed eddy current sensor", IEEE Transactions on Magnetics, 44(6), pp. 1638–1641, 2008. https://doi.org/10.1109/TMAG.2007.914846

[18] Abdou, A., Bouchala, T., Benhadda, N., Abdelhadi, B., Benoudjit, A. "Influence of conductive pollution on eddy current sensor signals", Russian Journal Nondestructive Testing, 54(3), pp. 192–202, 2018. https://doi.org/10.1134/S1061830918030026

[19] Burrascano, P., Cardelli, E., Faba, A., Fiori, S., Massinelli, A. "Numerical analysis of eddy current non-destructive testing (JSAEM Benchmark, Problem# 6–Cracks with different shapes)", In Proc. of the E'NDE Conference, Budapest, Hungary, Jun, 2000. [online] Available at: http://web.dibet.univpm.it/fiori/publications/ENDE00a.PDF [Accessed: 19 September 2024]

[20] Kuczmann, M., Iványi, A. "The finite element method in magnetics", Akadémiai Kiadó, 2008. ISBN 978 963 05 8649 8 https://doi.org/10.13140/2.1.3104.1927

[21] Bouillault, F., Ren, Z., Razek, A. "Calculation of 3D eddy current problems by an hybrid T-Omega method", IEEE Transactions on Magnetics, 26(2), pp. 478–481, 1990. https://doi.org/10.1109/20.106357